

Measurement of the L , M , N , O , and P electron densities at the Pt nucleus in the metallic Pt lattice

H. Daniel and M. Feil

Physics Department, Technical University of Munich, Munich, Germany

B. Martin

Max Planck Institute of Nuclear Physics, Heidelberg, Germany

(Received 8 March 1977)

The internal-conversion lines of s and p electrons from the L , M , N , O , and P shells of metallic platinum have been measured for the 31-keV $M1$ transition in $^{195}\text{Pt}^m$ with a high-resolution magnetic β -ray spectrometer; s -electron densities at the nucleus were deduced.

The determination of the densities of electrons from various outer shells at the nucleus is a problem which has been solved in some selected cases: self-consistent calculations are possible for free atoms and free ions,¹⁻² and experiments, particularly on ^{57}Fe , though difficult, have been performed.³⁻⁶ In the present paper we report on a measurement of s -electron densities at the nucleus in the case of Pt in the metallic Pt lattice. No experimental data or calculations are hitherto available for a heavy element in the condensed state.

It has been pointed out by a number of authors⁷⁻¹⁰ that the internal conversion coefficients for $M1$ transitions are to a very good approximation proportional to the electron density at the nucleus. Overlap and exchange effects which have not yet been calculated are believed to play a much smaller role than in electron capture.¹¹ This is most obvious for the overlap effect: the nuclear charge change in electron capture fully affects all atomic electrons while the charge change of the electron shell due to either electron capture or internal conversion strongly affects the electrons of more outward shells only. Another argument is the excellent agreement between experiment and present theory in the case of internal conversion in inner shells. Hence, high-resolution internal-conversion-electron spectroscopy is a very powerful tool, and indeed up to now the only tool for performing measurements which can lead to a determination of the outer-shell electron densities at the nucleus.

In Fig. 1 we illustrate this proportionality between electron contact density $\rho_n(0)$ of s electrons with the principal quantum number n and the internal-conversion coefficient β_n for $M1$ internal conversion of the same electrons. Data are shown for

various values of the atomic number Z and for various transition energies E . The electron densities were computed according to Liberman *et al.*,² and the internal-conversion coefficients according to Pauli and Raff.¹²

In the course of our experiments eight different sources of $^{195}\text{Pt}^m$ (4.1 d) ranging from 10 to 112 $\mu\text{g}/\text{cm}^2$ in thickness were used. They consisted of Pt metal (in some cases enriched to 83% in ^{194}Pt) evaporated *in vacuo* on quartz and then irradiated for 10 d, in the reactor FR2 in Karlsruhe, Germany. Electrostatically corrected broad sources (15 strips of 0.5 by 20 mm each) were used. Each source was reactivated between one and four times and then remeasured. The internal-conversion electron spectra were obtained with a $\frac{1}{2}\pi(13)^{1/2}$ high-resolution iron-free magnetic spectrometer¹³ using an anticoincidence-shielded proportional counter as the detector.¹⁴ Individual line intensities were extracted by computer analysis of the spectra.¹⁵ Figure 2 shows a typical spectrum with the individual line shapes as determined by the computer analysis. Table I summarizes the data on sources and runs.

Almost all the intensity of those conversion electrons which are ejected simultaneously with shake-off is in a rather short tail of the line.¹⁶ Therefore it is automatically included in the line intensity if the tail is included when determining the line intensity. In our evaluation of the experimental data we approximated the background, separated in a source-dependent part and a part not arising from the source, by a smooth function which was subtracted from the raw spectrum. The line intensity was then determined from the area of the remaining background-free spectrum. This procedure is reliable in the case of low, and well-

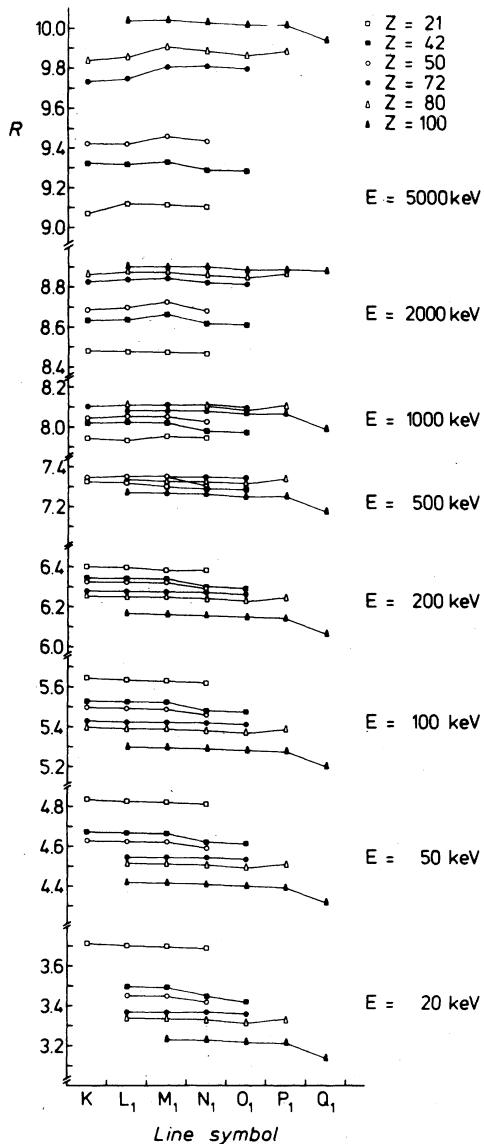


FIG. 1. Illustration of the proportionality between calculated values of electron contact density $\rho_n(0)$ and M1 conversion coefficient β_n . $R = \log_{10}[\alpha_0^3 \rho_n(0) / \beta_n]$ plotted versus n , the n values being symbolized by the conversion-line symbols, with a_0 meaning the Bohr radius.

approximated, background. In our spectrometer the background is low due to antiscattering baffles, an anticoincidence-shielded electron detector with subsequent pulse-height selection (proportional counter)¹⁴ and, of course, high resolution, and varies very smoothly with the spectrometer cur-

rent. In calculating the intensity ratios between lines all belonging to the *L*, *M*, or *N-O-P* "groups" no corrections due to source thickness effects were applied because the energies and line shapes are fairly similar within each group. The results for the line-intensity ratios are listed in Table III. For comparison results of earlier experimental work¹⁷⁻²⁰ and theoretical values²¹ for *M*1 with an admixture of $\delta^2 = 2 \times 10^{-4} E^2$ are included; our experiment yields $\delta^2 = (2.0 \pm 0.8) \times 10^{-4}$, in agreement with earlier work.²⁰

When comparing electron intensities of lines from different groups, the energy dependence of scattering and absorption also has to be taken into account. Multiple scattering leads to an increase in intensity at small thicknesses.²² The "increase" factor for normal-emission direction is given by the function $f_1(at_0)$ of Ref. 23 where a is the scattering constant and t_0 the source thickness. This factor was also used in our calculations since it does not strongly depend on the emission angle,²⁴ except for angles much larger than the ones used in this experiment. To keep within the region of validity for the theory, only sources up to $50 \mu\text{g}/\text{cm}^2$ were used for *L* conversion lines which are of low energy, while for higher lines all sources could be used. The factors $f_1(at_0)$ are listed in Table I. The resulting internal-conversion coefficients normalized to the theoretical value²¹ for the *M*1 electron line are given in column 2 of Table III. Allowance was made for an intensity error of 2%, the latter being due to the source thickness correction, and for an additional 2% caused by the change in line shape with energy. The reason one normalizes to the theoretical value of the *M*1 line is that the theory based on a free atom will give the correct internal-conversion coefficient for tightly bound electrons, and the experimental value is more accurate than for the *L*₁ line due to the smaller source thickness effect. Electron density values at the nucleus deduced from these experimental internal-conversion coefficients and values from Hartree-Fock-Slater calculations for the free atom² are listed in columns 4 and 5, respectively. The potential used² has contributions from the finite-size nucleus, from the Coulomb field of the electron charge distribution, and from "exchange," the latter being of the Slater " $\rho^{1/3}$ " type; more specifically, we used a Slater-type Kohn-Sham potential (i.e., the parameter² α taken to be $\frac{2}{3}$) with tail correction.

An inspection of Tables II and III shows good agreement between theory and the present experiment for the inner shells (*L*, *M*, and *N*) except for transitions involving $p_{3/2}$ electrons. The deviation in the latter case may very well be due to penetration effects¹⁹ as the regular *M*1 internal conversion of these electrons is very small. In the outer

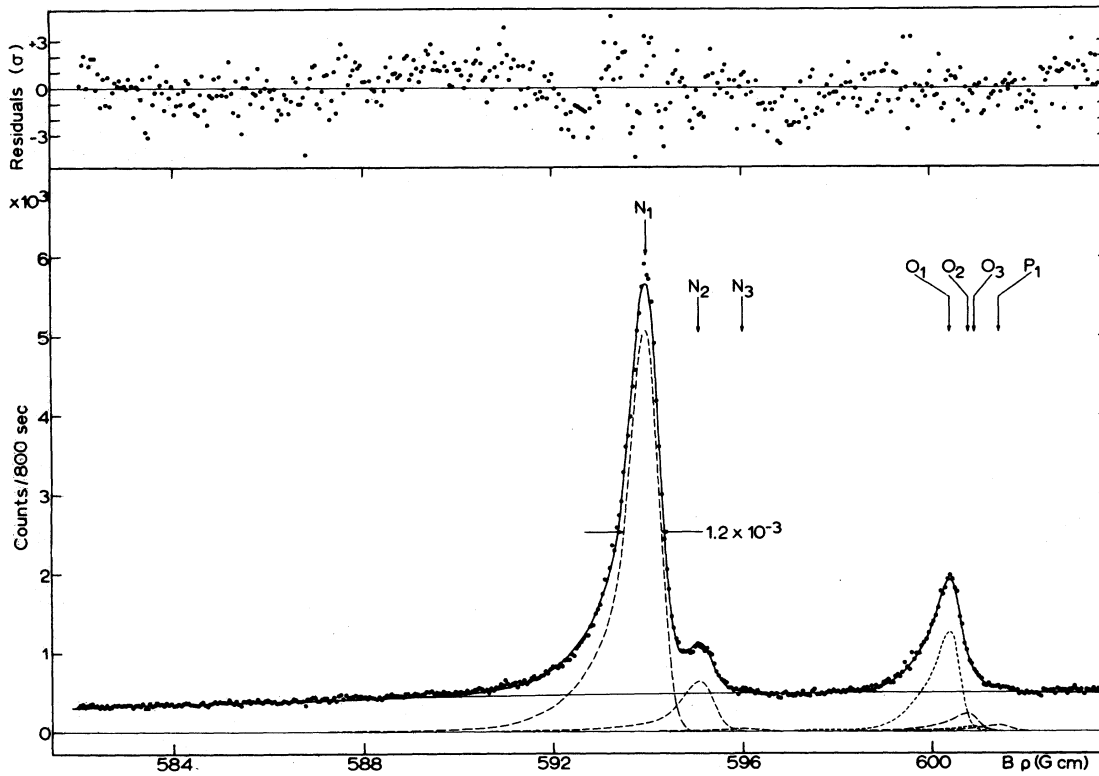


FIG. 2. N -, O -, P -conversion electron lines of the 30.876-keV M_1 transition in ^{195}Pt , intensity vs magnetic rigidity $B\rho$. The solid curve is the result of the least-squares fit yielding the components shown by dashed lines. The spectrum of residuals measured in standard deviations is given in the upper part of the figure.

shells (O and P), on the other hand, either there are differences (O_1 and O_{2+3}), or the agreement is meaningless. The difference in the case of O_{2+3} cannot be attributed to penetration as it is too

large and of different sign compared to M_3 and N_3 . The O_1 internal-conversion coefficient and, hence, the contact density are definitely smaller than those given by the free-atom calculation. The ratio be-

TABLE I. Sources, measured internal-conversion electron lines, and source thickness corrections $f_1(at_0)$.

Source No.	1	2	3	4	5	6	7	8
Thickness ($\mu\text{g}/\text{cm}^2$)	10	30	35	35	35	50	85	112
Enriched	no	no	no	yes	yes	no	no	no
Number of activations	2	5	5	4	4	3	4	3
Measured lines	L_1	L_1, L_2	L_1, L_2, L_3	L_1, L_2, L_3	L_1, L_2, L_3	L_1, L_2, L_3	M_1, M_2, M_3	M_1
	M_1	M_1, M_2, M_3	M_1, M_2, M_3	M_1, M_2, M_3	M_1, M_2, M_3	M_1, M_2, M_3	M_1, M_2, M_3	M_1
	N_1, N_2, N_3	N_1, N_2, N_3	N_1, N_2, N_3	N_1, N_2, N_3	N_1, N_2, N_3	N_1, N_2	N_1, N_2	N_1
		O_1, O_{2+3}	O_1, O_{2+3}	O_1, O_{2+3}	O_1, O_{2+3}	O_1, O_{2+3}	O_1, O_{2+3}	
		P_1		P_1				
$f_1(at_0)$					
L	1.06	1.07	1.07	1.07	1.07			
M	1.03	1.07	1.07	1.07	1.07	1.09	1.08	1.00
N	1.02	1.06	1.06	1.06	1.06	1.08	1.08	1.04
O, P	1.02	1.06	1.06	1.06	1.06	1.08	1.08	1.06

TABLE II. Experimental and theoretical internal-conversion coefficient ratios.

Ratio	This work	Ref. 17	Ref. 18	Ref. 19, 20	Theory (Ref. 21)
L_1/L_2	9.3 ± 0.4	12.8 ± 0.5	9.19 ± 0.29	9.17 ± 0.27	9.74
L_2/L_3	6.7 ± 0.4	5.82 ± 1.20	6.0 ± 2.4	6 ± 6	7.14
L_1/M_1	4.32 ± 0.13	4.99 ± 0.20	5.00 ± 0.28		4.36
M_1/M_2	9.00 ± 0.18	8.3 ± 1.0	8.3 ± 1.1	8.26 ± 0.41	9.00
M_2/M_3	9.5 ± 1.1			7.1 ± 1.8	7.11
M_1/N_1	4.10 ± 0.25	3.69 ± 0.30			3.95
N_1/N_2	8.8 ± 0.5				9.22
N_2/N_3	12 ± 5				7.31
N_1/O_1	5.9 ± 0.3	5.7 ± 1.7			5.08
O_1/O_{2+3}	3.4 ± 0.4				9.62
O_1/P_1	23 ⁺¹² ₋₃				24.6

tween the contact densities of *s* electrons in the metal and free atom (fa) states of a given *n*, is

$$\xi_n = \rho_n^{\text{metal}}(0) / \rho_n^{\text{fa}}(0).$$

Using the experimental value for the O_1 subshell given in Table III one obtains

$$\xi_5 = 0.82 \pm 0.05.$$

Although the theoretical and experimental P_1 internal-conversion coefficient and the contact density values are in agreement, there is experimental evidence that the electron configuration of Pt

metal strongly differs from the free-atom configuration $5d^96s^1$. If we write the metal configuration $5d^96s^{1-\eta}6(p+d+\dots)^\eta$, η can be estimated²⁵ to be around 0.7. With $\eta = 0.7$ we obtain

$$\xi_6 = 2.9^{+1.6}_{-1.0}.$$

ACKNOWLEDGMENT

We acknowledge the Gesellschaft für Kernforschung mbH, Karlsruhe, Germany, for the irradiation of the Pt metal.

TABLE III. Experimental and theoretical values for internal-conversion coefficients and electron densities.

Line	Conversion coefficient β_n		Electron density ^a $\rho_n(0)$	
	This work	Theory ^b	This work	Theory ^c
L_1	26.6 ± 0.8	26.85	(2.16 ± 0.06) × 10 ⁵	2.19 × 10 ⁵
L_2	2.88 ± 0.12	2.76		
L_3	0.433 ± 0.026	0.386		
M_1	6.154	6.154	4.99 × 10 ⁴	4.99 × 10 ⁴
M_2	0.684 ± 0.014	0.683		
M_3	0.072 ± 0.008	0.096		
N_1	1.50 ± 0.06	1.56	(1.22 ± 0.05) × 10 ⁴	1.27 × 10 ⁴
N_2	0.170 ± 0.009	0.169		
N_3	0.014 ± 0.006	0.023		
O_1	0.252 ± 0.015	0.307	(2.04 ± 0.12) × 10 ³	2.49 × 10 ³
O_{2+3}	0.075 ± 0.009	0.032		
P_1	0.011 ^{+0.006} _{-0.004}	0.0125	(0.9 ^{+0.5} _{-0.3}) × 10 ²	1.01 × 10 ²

^aIn units of a_0^{-3} , a_0 being the Bohr radius.

^bReference 21.

^cReference 2.

- ¹D. Liberman, J. T. Waber, and D. T. Cromer, *Phys. Rev.* **137**, A27 (1965).
- ²D. A. Liberman, J. T. Cromer, and J. T. Waber, *Computer Phys. Commun.* **2**, 107 (1971).
- ³F. T. Porter and M. S. Freedman, *Phys. Rev. C* **3**, 2285 (1971).
- ⁴T. Shinohara and M. Fujioka, *Phys. Rev. B* **7**, 37 (1973).
- ⁵T. Shinohara, M. Fujioka, H. Onodera, K. Hirstake, H. Yamamoto, and H. Watanabe, *J. Phys. (Paris) C* **6**, 215 (1974).
- ⁶B. Martin and R. Schulé, *Phys. Lett. B* **46**, 367 (1973).
- ⁷H. Daniel, *Z. Phys.* **223**, 150 (1969).
- ⁸U. Raff, K. Adler, and G. Baur, *Helv. Phys. Acta* **45**, 427 (1972).
- ⁹M. Fujioka, U.S.-Japan Joint Seminar on Hyperfine Interactions Involving Excited Nuclei, 1972, quoted in Ref. 5.
- ¹⁰H. C. Pauli, K. Alder, and R. M. Steffen, *The Electromagnetic Interaction in Nuclear Spectroscopy*, edited by W. D. Hamilton (North-Holland, Amsterdam, 1975), p. 341 ff.
- ¹¹G. T. Emery, *Ann. Rev. Nucl. Sci.* **22**, 165 (1972).
- ¹²H. C. Pauli and U. Raff, *Computer Phys. Commun.* **9**, 392 (1975) and (private communication).
- ¹³H. Daniel, P. Jahn, M. Kuntze, and B. Martin, *Nucl. Instrum. Methods* **82**, 29 (1970).
- ¹⁴B. Röde, *Z. Naturforsch. A* **29**, 261 (1974).
- ¹⁵D. Merkert, R. Schulé, and B. Martin, Report No. MPI H-1973-V 33 (Max Planck Institute of Nuclear Physics, Heidelberg, Germany, 1973) (unpublished).
- ¹⁶F. T. Porter, M. S. Freedman, and F. Wagner, *Phys. Rev. C* **3**, 2246 (1971).
- ¹⁷L. H. Toburen and R. G. Albridge, *Z. Phys.* **240**, 185 (1970).
- ¹⁸B. Ahlesten and A. Bäcklin, *Nucl. Phys. A* **154**, 303 (1970).
- ¹⁹H. H. Hsu and G. T. Emery, *Bull. Am. Phys. Soc.* **17**, 606 (1972), and as quoted in Ref. 20.
- ²⁰M. J. Martin, *Nucl. Data Sheets B* **8**, 431 (1972).
- ²¹Program CATAR (Ref. 12) with atomic wave functions from Ref. 1.
- ²²D. Fehrentz and H. Daniel, *Nucl. Instrum. Methods* **10**, 185 (1961).
- ²³H. Daniel, O. Mehling, O. Müller, P. Schmidlin, H. Schmitt, K. S. Subudhi, and E. Neuburger, *Nucl. Phys.* **45**, 529 (1963).
- ²⁴H. Paul, *Nucl. Instrum. Methods* **37**, 109 (1965).
- ²⁵W. Rügge, *Helv. Phys. Acta* **46**, 735 (1974).